Asociación Argentina
de Mecánica Computacional

Mecánica Computacional Vol XXIX, págs. 7835-7856 (artículo completo)
Eduardo Dvorkin, Marcela Goldschmit, Mario Storti (Eds.)
Buenos Aires, Argentina, 15-18 Noviembre 2010

ANALYSES OF OFFSHORE SYSTEMS WITH SELECTIVE ACTIVATION OF FINITE ELEMENTS

Bruno Martins Jacovazzo[a], **Breno Pinheiro Jacob**[b]

[a]*Centro de Tecnologia, UFRJ, Cidade Universitaria, Ilha do Fundao – RJ, Bloco I, Sala 120 Subsolo, Cep 21949900, Caixa Postal 68506, Brasil, bruno@lamcso.coppe.ufrj.br, http://www.lamcso.coppe.ufrj.br*

[b]*Centro de Tecnologia, UFRJ, Cidade Universitaria, Ilha do Fundao – RJ, Bloco I, Sala 120 Subsolo, Cep 21949900, Caixa Postal 68506, Brasil, breno@lamcso.coppe.ufrj.br, http://www.lamcso.coppe.ufrj.br*

Keywords: Activation, Deactivation, Finite Elements, Offshore, Numerical Simulation.

Abstract. Several procedures that are executed in offshore environment involve the coupling and decoupling of cables, payment and collect of lines. Moreover, some offshore structures can suffer from fails in the systems that guarantee their average positioning as, for example, the rupture of floating platforms mooring lines.
In general, these structures are dynamically simulated through numerical tools based at the Finite Elements method. Situations where meshes must be added or removed from dynamic simulations are commonly carried through the division of the numerical model in stages, losing, when it is relevant, information of the structure behavior during the transition from a situation to another.
This work presents two studies of real offshore systems cases involving a numerical tool that has been developed with the capacity to add or to remove finite elements during the execution of a numerical simulation. The first case presents a typical model of a semi-submersible platform in which the rupture of a line from its mooring system occurs due to the action of environmental load effects. The second one analyzes a pipeline that is going to be laid on the seabed through the Floating Spiral method, at the stage in which its last wrap is ready to be unwound. At this stage, a cable system proposed in order to guarantee the control and the security of the operation is sequentially decoupled and the stresses acting on the pipeline are verified.

1 INTRODUCTION

The objective of this paper is to evaluate the capacity of a numerical program to simulate real offshore cases involving the activation or rupture of system lines. Such situations may occur in installation or operational procedures, involving the coupling and decoupling of cables, payment and collecting of mooring lines of floating platform, launching of a pipeline or subsea equipment, and so on.

Moreover, in some situations the offshore structures can suffer accidents that lead to the failure in the systems that guarantee their average positioning as, for example, the rupture of a line of the mooring system of a floating platform.

In general, these situations are dynamically simulated through numerical tools based on the Finite Element method. Such situations, where meshes must be added or removed from dynamic simulations, are commonly carried through the division of the numerical model in stages, losing, when it is relevant, information of the structure behavior during the transition from a situation to another.

Therefore, in order to numerically represent the activation and deactivation of lines, a numerical tool for the selective activation of finite elements during the execution of dynamic offshore simulations has been developed. This numerical tool has already been presented in detail in another paper (Jacovazzo and Jacob, 2009) and its main characteristics are summarized in this paper at Section 2.

This tool is implemented in the SITUA-Prosim program, which has been developed since 1997 (Jacob, 2006) in cooperation by Petrobras and LAMCSO/COPPE. This program performs coupled static and dynamic nonlinear analyses for a wide range of offshore operations.

While the former paper dealt basically with academic examples, this paper now focuses on two real offshore situations. The first one simulates the rupture of a mooring line that could be occasioned by an extreme load condition acting on the platform. The second simulates an operational procedure of pipe laying through the Floating Spiral method (Silva et al., 2008; Jacovazzo et al., 2008) in which a cable system is sequentially disconnected to the pipeline in order to guarantee a controlled unwind process for the Floating Spiral.

2 SELECTIVE ACTIVATION OF FINITE ELEMENTS

The numerical tool considered here takes advantage of two peculiarities in the code structure of the SITUA-Prosim program. The first one is related to the non-linear effects of the analysis, demanding the program to constantly recalculate the matrices that represent the numerical problem. Usually, these matrices are recalculated on each Newton-Raphson iteration (Bathe, 1996; Jacob and Ebecken, 1994). The second one is related to the calculation of the elements contribution to the analysis, which is made in a local level and then is spread to the global level.

Each element of the mesh is associated to an activation and deactivation function, which defines the time steps that an associated element is going to be activated, deactivated or in a transient phase. During the execution of a numerical simulation, the program verifies, in each time step, which is the activation state of a particular element and then defines a factor that is a number between “zero” and “one”.

If the particular element is activated for the current time step, its multiplication factor equals to “one” and, during the spreading process, its contribution is completely considered to fill the global matrices of the problem. If this element is in a transient phase, its multiplication factor is defined as a number between “zero” and “one” and its contribution is multiplied by

this factor before being spread on the global matrices of the problem. If the element is deactivated, its contribution is not considered and its multiplication factor equals to "zero". The activation and deactivation functions must be defined for the entire simulation length. This procedure is represented at the local level by the flowchart illustrated in Figure 1.

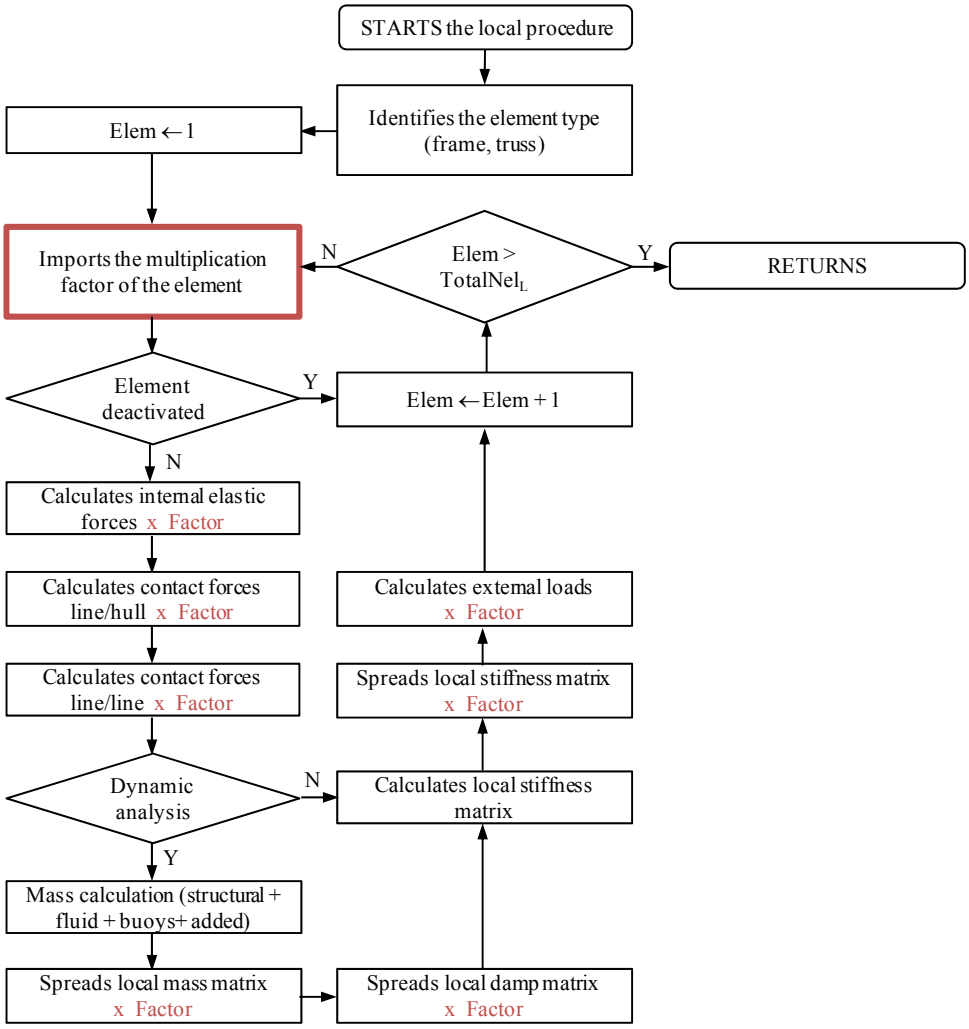

Figure 1: Application of the multiplication factor

3 MOORING LINE RUPTURE

3.1 Problem description

In usual design situations, the line rupture simulations are performed simply removing the Finite Elements mesh that represents it even before the beginning of the simulation. After a considerable time, the mean values of the platform motions and line tensions are statistically equal to the mean values obtained with a simulation in which the rupture of a line is performed after its start.

However, in some situations it is necessary to evaluate the transient effects in the model that occur right after the rupture of a line. In such cases, the line should be disrupted during the execution of the simulation.

An example of case that such procedure is considered necessary is the one in which support structures are anchored very close to production platforms in order to perform temporary services. In such case there is a possibility to occur a collision between these

structures due to the transient effects occasioned by a mooring line rupture.

Specifically in this paper, the presented study case main objective is to evaluate if the elements deactivation tool is prepared to analyze a real project case. The proposed model to this task is a production platform in which its mooring system is analyzed with the incidence of an environmental load. After performing a dynamic simulation of the intact system, two dynamic simulations were performed in order to evaluate the system behavior after the rupture of a mooring line.

This procedure was carried through two different ways. In the first one, the line was simply removed from the simulation even before its beginning. In the second one, the line was deactivated during the execution of the dynamic simulation.

3.2 Platform characteristics

The floating unit that was used in this example is a semi-submersible platform that had been standardized in the 17th Ocean Engineering Committee ITTC (Takezawa et al., 1985; Matao et al., 1985). This platform was numerically represented by the hybrid hydrodynamic model of the SITUA-Prosim software and it was headed towards the global "X" axis with a 20m draft. The global system is Cartesian and was placed at the still water level (SWL).

The main characteristics of the platform are described in Table 1. Figure 2 shows the floating unit modeled in the numerical program. In this model, the global coordinate system coincides with the structural coordinate system of the platform, except for the height difference given by the platform draft.

Parameter	Value	Unit
Length	115.00	m
Draft	20.00	m
Breadth	60.00	m
Height	43.00	m
Longitudinal center of gravity	0.00	m
Transversal center of gravity	0.00	m
Vertical center of gravity	17.50	m
Radius of gyration (Roll)	34.30	m
Radius of gyration (Pitch)	35.58	m
Radius of gyration (Yaw)	40.58	m
Displacement	34157	t

Table 1: Platform characteristics

The influence of the current and wave on the hull members are calculated through the Morison formulation (Morison et al., 1950). Second order effects have been ignored since the objective of this analysis is just to evaluate the deactivation elements tool in a project case and not to represent a real platform hull.

The wind effects are calculated based on the lateral projection of platform, adopted as 2000m² to any direction of load incidence.

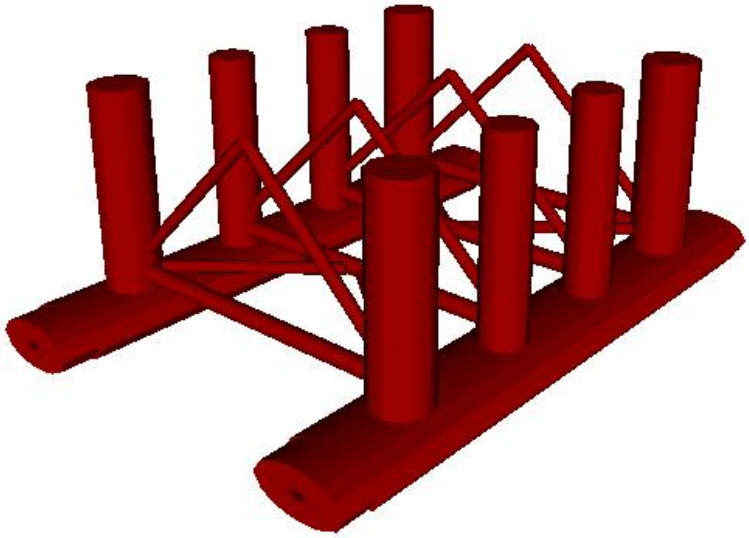

Figure 2: Numerical model of the platform

3.3 Lines

The system lines, including the risers and the mooring lines, are modeled by meshes of truss elements, with a constant element length of 5m.

Three types of steel catenary risers (SCR) have been employed in this model: 6, 8 and 10 inches. The main characteristics of the risers are described in Table 2. The mooring lines have been modeled as conventional catenary lines composed by two sections of chain (top and bottom) and by an intermediate section of steel wire rope. Their main characteristics are described in Table 3. The risers and mooring lines have been placed on the hull in a symmetric way. The risers model is described in Table 4 while the mooring lines model is described in Table 5.

Material	Φext (m)	Φint (m)	ν	E (kN/m²)	γ (kN/m³)	γ internal fluid (kN/m³)	CM	CD	HD (m)
SCR 6"	0.1715	0.1334	0.3	207000000	77	8	2	1.2	0.1715
SCR 8"	0.2223	0.1842	0.3	207000000	77	8	2	1.2	0.2223
SCR 10"	0.2731	0.2350	0.3	207000000	77	8	2	1.2	0.2731

Table 2: Risers material properties

Material	Φext (m)	EA (kN)	EI (kN*m²)	GJ (kN*m²)	MBL (kN)	Wair (kN/m)	Wwater (kN/m)	CM	CD	HD (m)
R4 Stud Chain	0.058	345483	1	0.7	3628	0.7227	0.627	2	1.7	0.102
EEIPS Steel Wire Rope	0.071	158302	0.7	0.5	3530	0.204	0.1694	2	1.2	0.071

Table 3: Mooring lines material properties

Riser	Material	Top Angle (deg)	"X" Angle (deg)
1	SCR 6"	9	80
2	SCR 8"	9	85
3	SCR 10"	9	90
4	SCR 8"	9	95
5	SCR 6"	9	100
6	SCR 6"	9	260
7	SCR 8"	9	265
8	SCR 10"	9	270
9	SCR 8"	9	275
10	SCR 6"	9	280

Table 4: Risers distribution at the platform

Line	Pre-Tension (kN)	"X" Angle (deg)	Top chain length (m)	Steel cable length (m)	Bottom chain length (m)
1	500	40	50	300	900
2	500	50	50	300	900
3	500	130	50	300	900
4	500	140	50	300	900
5	500	220	50	300	900
6	500	230	50	300	900
7	500	310	50	300	900
8	500	320	50	300	900

Table 5: Mooring lines distribution at the platform

3.4 Environmental data

The sea depth of this model was adopted as 200m and the seabed was considered flat. In order to perform this simulation, it has been adopted an extreme load condition with the following specifications: decenary current (Table 6), centenary wave (Table 7) and centenary wind (Table 8). The angles of attack and incidence are referred to the global system of coordinates.

Depth (m)	Velocity (m/s)	Angle of attack (deg)
0	0.82	45
20	0.82	45
80	0.42	45
95	0.37	45
100	0.00	45
200	0.00	45

Table 6: Current load

Parameter	Value
Spectrum	Jonswap
Hs (m)	7.84
Tp (s)	15.55
γ	1
Number of components	200
Angle of incidence (deg)	225

Table 7: Wave load

Parameter	Value
Type	Constant
Mean velocity in 10 minutes (m/s)	31.58
Angle of incidence (deg)	225

Table 8: Wind load

3.5 Model Visualization

Figures 3, 4 and 5 illustrate some views of the system modeled in the SITUA-Prosim software.

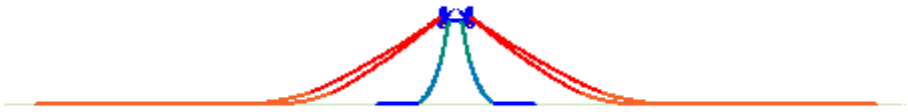

Figure 3: Model visualization – frontal view

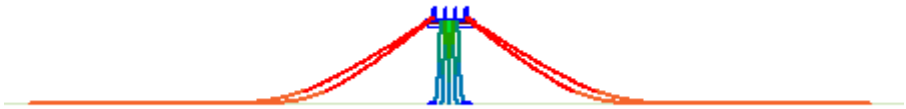

Figure 4: Model visualization – lateral view

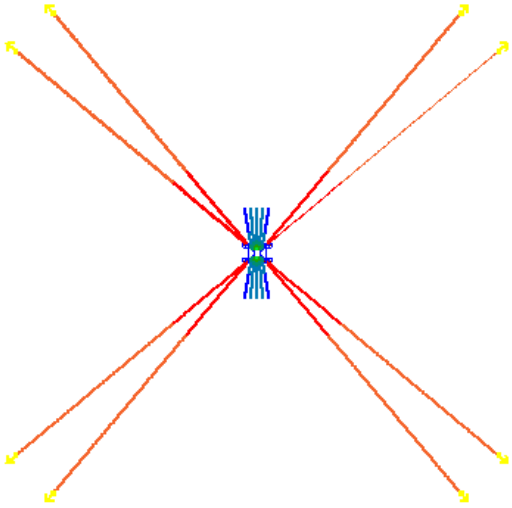

Figure 5: Model visualization – top view

3.6 Results

As can be seen in Table 7, the adopted wave load condition is an irregular sea state. Therefore, in order to evaluate the results, it was necessary to make a statistical approach.

As described before, the proposed model was first dynamically simulated considering an intact mooring system. It was observed that the platform offset had been reached 9.67% of the water depth. The most tensioned mooring line was line 05, with a statistical top tension of 1843.7kN, which equals to 50.82% of the chain MBL. This value is lower than the maximum tension specified by API RP 2SK (2006), which is 60% of the MBL. The second line with the highest tension level was line 06 with a statistical top tension of 1831.8kN. These results are presented in tables 9 e 10.

Since the design criteria for the intact model has not been violated, the simulations considering the rupture of the most tensioned mooring line have been performed. In the simulation in which the mooring line was disrupted after its beginning, the deactivation of line 05 had been performed with 300s. The results are presented in tables 9 e 10. As it can be observed, the design criteria for the lines still were not violated, since API RP 2SK specifies that the maximum tension in this case should not be higher than 80% of the line MBL.

Model	Maximum offset (m)	% Water Depth
Intact	19.33	9.67%
Line 05 deactivated	29.70	14.85%
Line 05 disrupted	29.69	14.85%

Table 9: Maximum statistical offsets values for the platform

Line	Intact		Line 05 deactivated		Line 05 disrupted	
	Max (kN)	% MBL	Max (kN)	% MBL	Max (kN)	% MBL
1	361.6	9.97%	206	5.68%	207.2	5.71%
2	367.3	10.12%	208.3	5.74%	216.7	5.97%
3	587.5	16.19%	617.1	17.01%	618.7	17.05%
4	680.3	18.75%	775.7	21.38%	779.7	21.49%
5	1843.7	50.82%	-	-	-	-
6	1831.8	50.49%	2790.5	76.92%	2788.8	76.87%
7	649.6	17.90%	638.9	17.61%	633.3	17.46%
8	576.2	15.88%	514.5	14.18%	511.3	14.09%

Table 10: Maximum statistical tensions values at the mooring line system

The figures below present the response series of some platform degrees of freedom considering a window of time near to the rupture of the mooring line. Specifically, the Figure 6 presents the offset response series, the Figure 7 presents the roll response series and the Figure 8 presents the pitch response series. The other degrees of freedom have not been illustrated in this paper due to space issues.

Also, the Figure 9 presents the tension response series for the second most tensioned mooring line of the system (line 06).

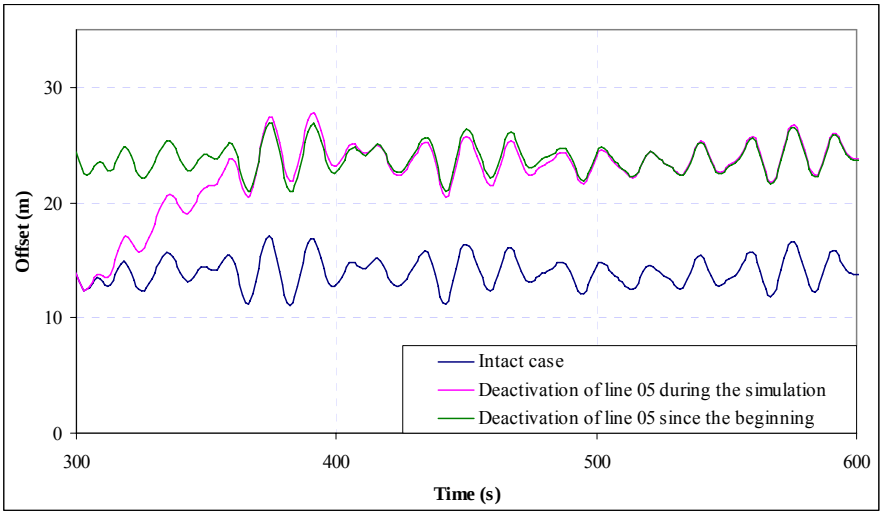

Figure 6: Platform offset response – 300s to 600s window

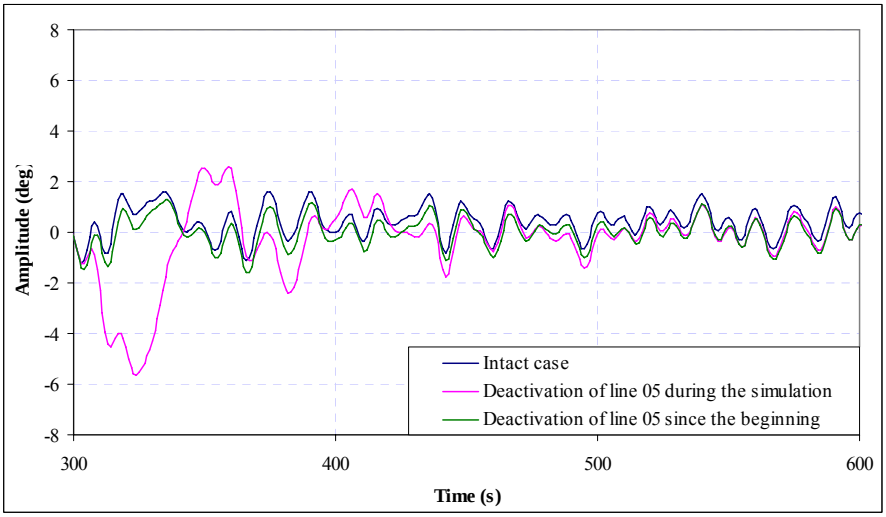

Figure 7: Platform roll response – 300s to 600s window

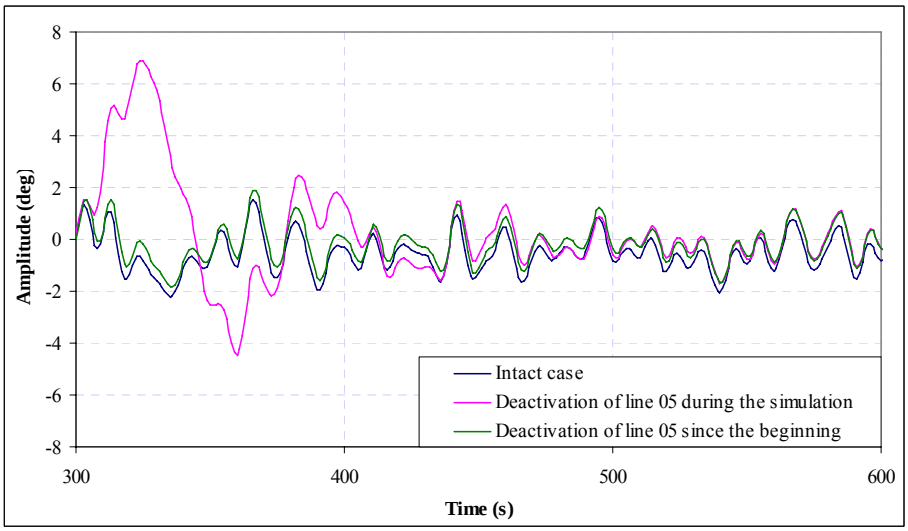

Figure 8: Platform pitch response – 300s to 600s window

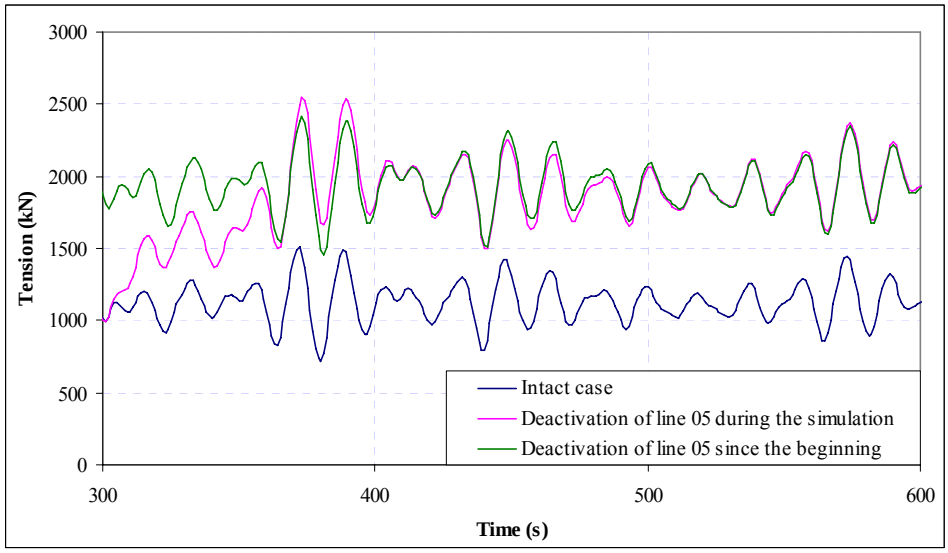

Figure 9: Tension of line 06 response (second line with the highest tension level) – 300s to 600s window

3.7 General Comments

The presented results demonstrate the efficiency of the Elements Deactivation tool that has been implemented in the software. The response series considering the model in which the line 05 was deactivated during the execution of the simulation initially followed the response series of the intact model. After that, with the deactivation of line 05, these series were affected by a transient effect and then started to follow the response series of the model in which the line 05 had been removed from the model before the beginning of the numerical simulation.

It can be observed in tables 9 e 10 that the statistical differences between the results of both rupture simulations were insignificant, as it was expected. However, when the simulation focus is to evaluate the transient effect occasioned due to the rupture of the line, the implemented tool becomes very important.

It should be emphasized that structures employing other types of mooring systems such as "taut-leg" and tension leg platforms (TLP) may lead to completely different results in which the transient effects can be much more expressive since these kind of structures are supported by very stiff mooring systems.

4 CONTROLLED UNWINDING PROCESS FOR THE FLOATING SPIRAL METHOD

4.1 Problem description

This project case shows the application of the element deactivation tool in multiple lines and different times of a dynamic numerical simulation.

In the Floating Spiral method of pipe laying, the pipeline is fabricated onshore in a shipyard protected by breakwaters. The welding process is made in structures placed on the land, under well controlled conditions and relatively relaxed time constraints. Therefore the welds can be better inspected, which allows for optimal control of quality in pipeline manufacturing. After passing the welding station, the pipeline is launched in the water, making use of a proper buoyancy reserve or assisted by the use of buoys.

The floating pipe is led by tugboats and guided by piles settled in the water to form a huge

spiral, as it can be observed in Figure 10. While the pipeline is being wound, clamps are placed to hold the spiral tightly, as it can be observed in Figure 11.

After assembling the pipeline into a huge floating spiral, an internal cable system is placed, the piles are removed and the system is towed to the installation site by tugboats.

After towing the Floating Spiral to the installation site, the pipe lay procedure is carried through by tugboats that unwind the pipeline in a pre-determined route. This process is performed through the gradually rupture of the clamps that hold two adjacent wraps of the Floating Spiral together. At the same time, the buoys that give buoyancy to the pipeline are removed and the pipeline is then laid on the seabed. The unwinding process of the Floating Spiral follows a constant and controlled procedure. The system is unwound in stages corresponding to the arc length between two consecutive clamps.

However, during the unwinding process of the last wrap of the Floating Spiral, all the clamps have been removed. Without an adequate procedure of operational safety, the last wrap of the Floating Spiral will be free to unwind, liberating a considerable accumulated energy abruptly.

To perform the unwinding process in a controlled way, an internal cable system has been proposed. This cable system, shown in Figure 12a, is sequentially disrupted during the process, allowing the Floating Spiral to be unwound in a gradual and controlled way.

To simplify the explanation of the process, only the last wrap of the spiral is graphically represented in all the cases of Figure 12. However, at this point of the operation procedure, all the other wraps of the spiral have already been unwound and the most of the pipeline length is resting on the seabed.

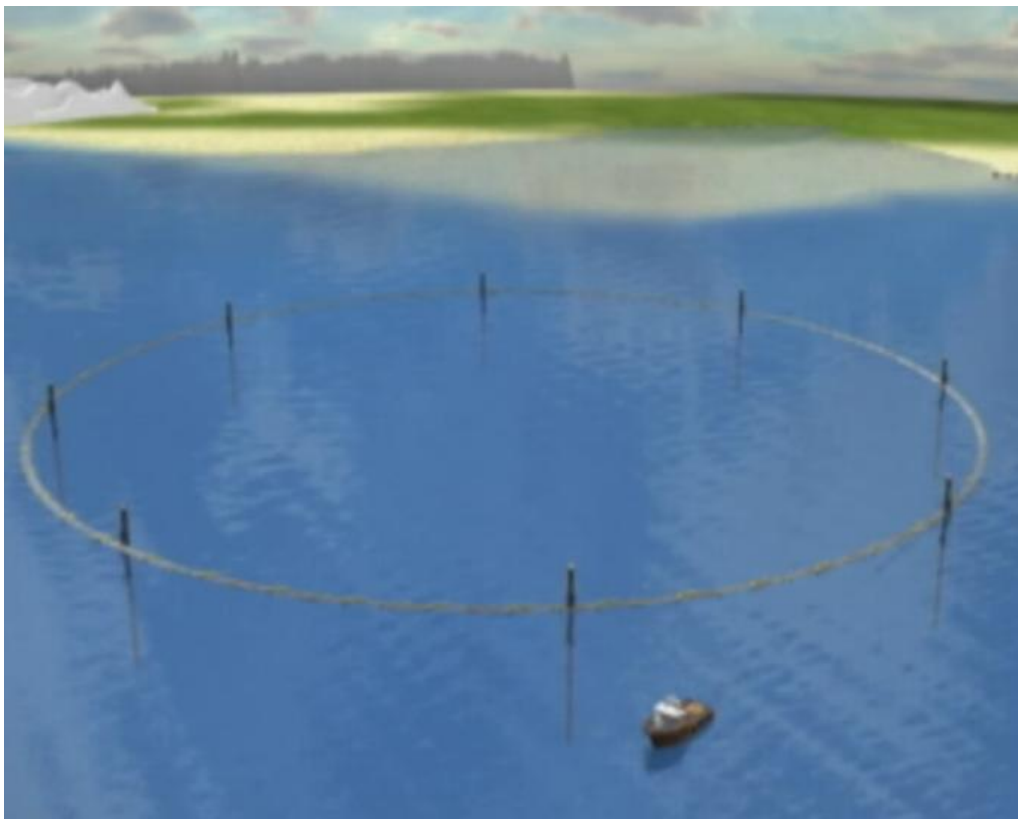

Figure 10: Floating Spiral being wound by a tugboat

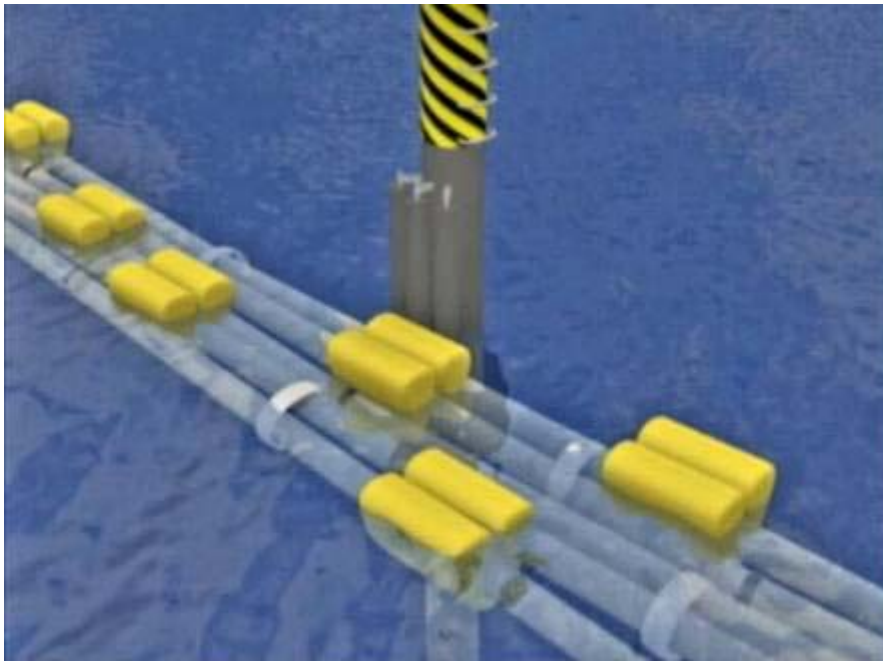

Figure 11: Detail of the pipeline clamps

The first stage of the controlled unwinding process of the Floating Spiral consists in the rupture of the last clamp that keeps the pipe wound. Then, the pipe starts to unwind and assumes the configuration presented in Figure 12b, in which the cables 1 and 3 are the most tensioned ones. It can be observed that the cable 2 keeps without being tensioned and assumes any configuration.

After that, in a second stage, the cable 1 is disrupted and the pipeline assumes the configuration presented in Figure 12c, in which the cables 2 and 3 are tensioned. Then, in a third stage, the cable 2 is disrupted and the pipeline assumes the configuration presented in Figure 12d. Finally, in the last stage of the process, the cable 3 is disrupted and the pipeline unwinds freely until it assumes a straight configuration. In this last stage, the elastic energy of the pipeline is considerably small, making the unwinding process to occur in a very slowly way. At this point, the unwinding process may be assisted by the tugboats.

The main objective of this numerical simulation is to reproduce this operation and verify the stresses acting on the pipeline and the corresponding tensions on the cable system.

4.2 Numerical simulation characteristics

To numerically represent this installation procedure, a dynamic numerical simulation has been performed in which the last clamp and the internal cable system that has been proposed were gradually deactivated. The considered simulation length in this case was 8000s and the time step of the dynamic simulation was 0.05s. To perform this numerical simulation, it has been employed the element deactivation tool that had been implemented in the software before.

The first stage, in which the last clamp of the Floating Spiral was deactivated, has been performed with 10s of simulation length. The second stage, in which the system assumed the configuration presented in Figure 12b and the cable 1 was deactivated, has been performed with 2000s of simulation length. The third stage, in which the system assumed the configuration presented in Figure 12c and the cable 2 was deactivated, has been performed with 4000s of simulation length. The fourth stage, in which the system assumed the configuration presented in Figure 12d and the cable 3 was deactivated, has been performed

with 6000s of simulation length. Finally, in the fifth and last stage, the pipeline was freely unwound and, in the end of the numerical simulation, with 8000s of simulation length, the pipeline assumed the configuration presented in Figure 12e. As it can be observed, this simulation length was still insufficient to completely unwind the pipeline.

4.3 Pipe properties

The simulated pipeline had an 8 inch diameter section and was made of an X60 steel, which properties are given by API 5L (2000). The pipeline main characteristics are presented in Table 11.

To numerically represent this pipeline, it has been employed tridimensional frame elements in the model. These elements were modeled with 2m length, which corresponds to 1% of the Floating Spiral diameter, that is 200m. The stresses acting in the external wall of the pipeline in the beginning of the numerical simulation correspond to 55% of its yield stress. This state of stress only occurs due to the fact that the pipeline was wound with the presented diameter.

In order to simplify the model, all the section of the pipeline that would be already in a straight configuration and possibly would be already resting on the seabed was not modeled. Then, the extremity node that would be linked to this section of the pipeline that has not been represented was restrained.

The SITUA-Prosim software is provided with a wizard module to automatically calculate the initial curvature of the pipeline based on the Floating Spiral diameter. This initial curvature is used to apply initial moments to the model that give the unwinding tendency to the pipeline.

Parameter	Value	Unit
Weight in air	0.6340	kN/m
Buoyancy	0.3791	kN/m
Nominal diameter	8	in
External diameter (API 5L)	8.625	in
Internal diameter (API 5L)	7.635	in
Elasticity modulus	2.07×10^8	kN/m^2
Specific weight	77	kN/m^3
Yield stress (API 5L)	414000	kN/m^2

Table 11: Pipeline properties

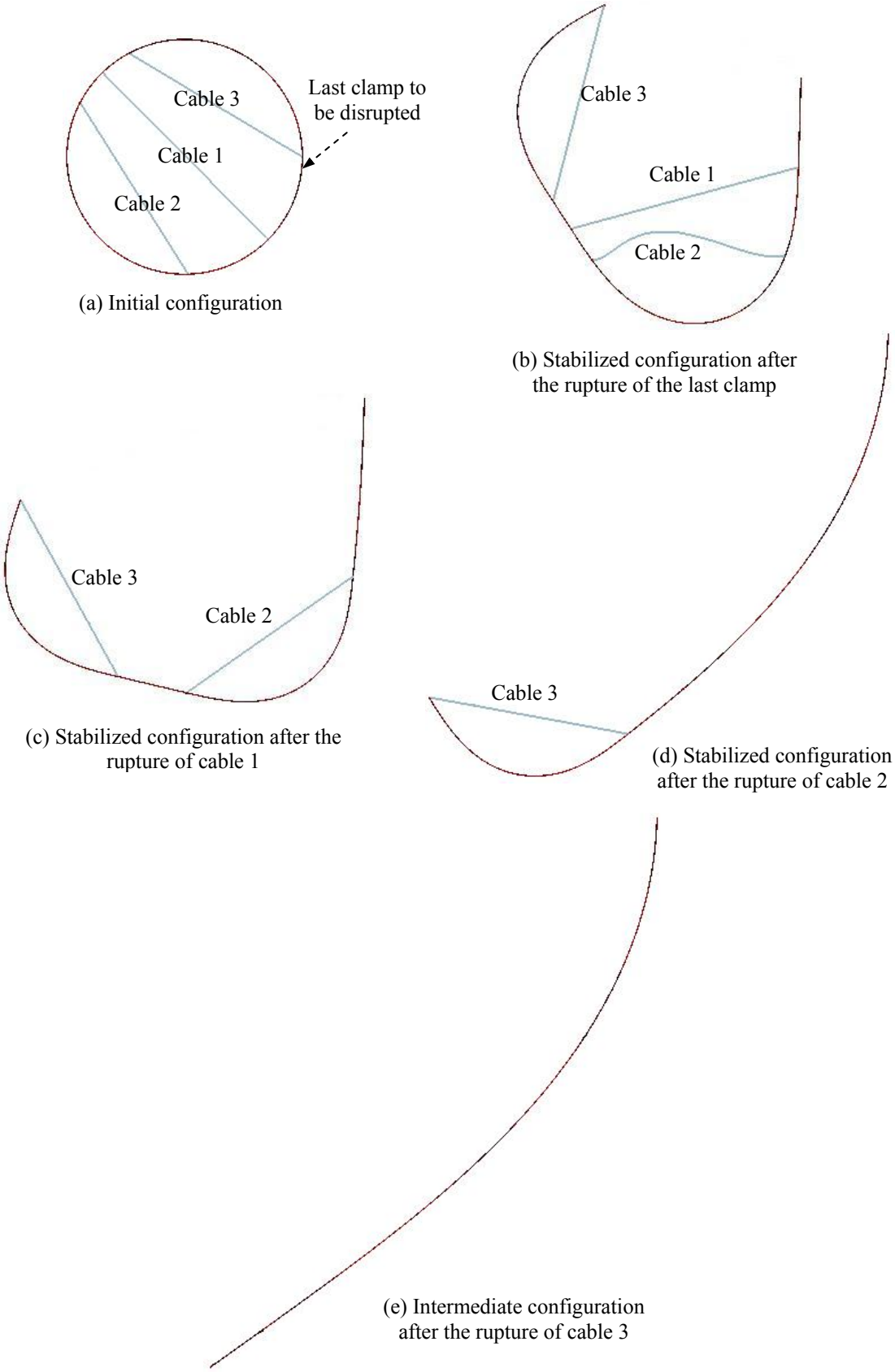

Figure 12: Controlled unwinding process stages – superior view

4.4 Buoyancy system

As can be observed in Table 11, the pipeline was not provided with a proper buoyancy capacity itself. In this case, distributed buoys have been adopted to give a buoyancy reserve to the pipeline of 10% of its weight. Then, after adding the buoys to the model, the pipeline weight in the water was modified to -0.0634kN/m and its hydrodynamic diameter was modified to 0.297m.

Figure 13 shows a detail of the tridimensional numerical model, in which it is possible to identify the small amount of buoyancy of the pipeline with the distributed buoys.

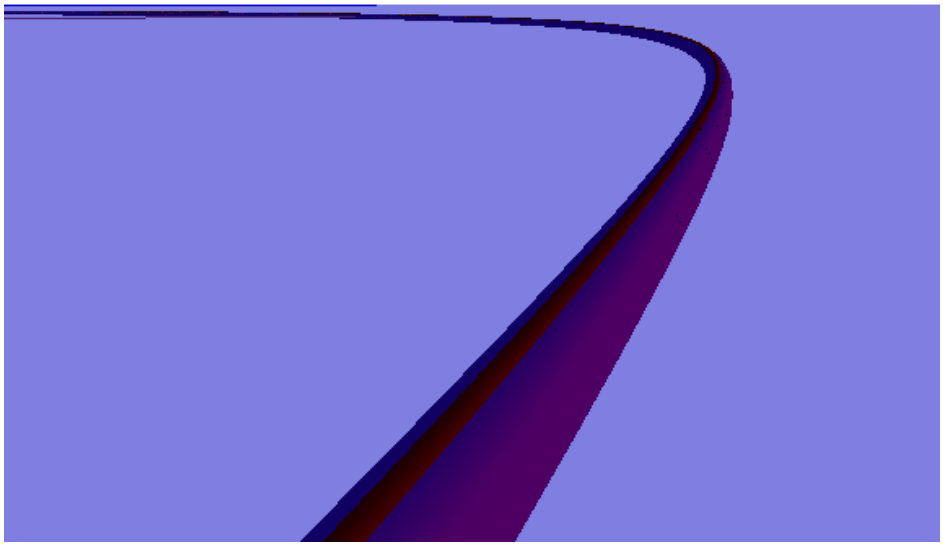

Figure 13: Detail of the numerical model – buoyancy capacity of the pipe

4.5 Cable system

To numerically represent the cable system, tridimensional frame elements are employed in the model. This system is composed by three polyester cables, which the properties are presented in Table 12.

Parameter	Value	Unit
Material	Polyester	-
External diameter	0.122	m
Axial stiffness	19502	kN
Flexional stiffness	0.7	kNm²
Torsional stiffness	0.5	kNm²
Minimum breaking load (MBL)	3924	kN
Weight in air	1.00E-04	kN/m
Weight in water	1.00E-05	kN/m
Inertia coefficient	2	-
Drag coefficient	1.2	-
Hydrodynamic diameter	0.122	m

Table 12: Cable system properties

4.6 Environmental load

In this simulation, it was not considered any environmental load acting on the structure. The objective is to analyze the stresses acting in the pipeline and the tensions acting in the cable system only considering the unwinding process of the Floating Spiral.

4.7 Results

The results presentation has been organized in order to show the Von Mises stresses acting in the pipeline external wall for each one of the unwinding stages of the last wrap of the Floating Spiral.

In order to make the results more comprehensive, all the figures below have been provided with 100%, 80% and 55% levels of the X60 steel yield stress. The value of 80% of the yield stress corresponds to the maximum recommended by API RP 2RD (1998). The value of 55% of the yield stress corresponds to the level of stress acting in the pipeline external wall, only due to the fact that the pipeline was wound with a 200m diameter. The figures below are also provided with vertical dashed lines, indicating the connection points of the cables on the pipeline. These vertical lines are numbered according to the schematic figure in each graph.

It is important to emphasize that the Figure 12 shows the deformed configurations of the model besides demonstrating the operation procedures in Item 4.1.

The Figure 14 presents the Von Mises stresses acting in the pipeline external wall in the beginning of the numerical simulation (configuration presented in Figure 12a). The Figure 15 presents the Von Mises stresses acting in the pipeline external wall immediately before the deactivation of cable 1 (configuration presented in Figure 12b). The Figure 16 presents the Von Mises stresses acting in the pipeline external wall immediately before the deactivation of cable 2 (configuration presented in Figure 12c). The Figure 17 presents the Von Mises stresses acting in the pipeline external wall immediately before the deactivation of cable 3 (configuration presented in Figure 12d). The Figure 18 presents the Von Mises stresses acting in the pipeline external wall after 8000s of numerical simulation and all cables deactivated (configuration presented in Figure 12e). Finally, the Figure 19 presents the pipeline external wall envelope of stresses, considering all the simulation time. The curves are generated along the pipeline length, counting from its free to its restrained extremity, anticlockwise.

The Figure 20 presents the tension series of the cable system. It can be observed that the cable 1 generates results until 2000s of simulation time, which is the time that this cable was deactivated. The cable 2 generates results until 4000s of simulation time and cable 3 generates results until 6000s of simulation time, following the same analogy.

4.8 General Comments

Considering this project example, the elements deactivation tool has demonstrated itself very useful and efficient in performing this kind of dynamic numerical simulation.

In the beginning of the simulation, according to the graph that has been shown in Figure 14, the stresses acting in the pipeline were constant at the level of 55% of its yield stress. This level of stress, as described before, corresponds to the stresses assumed by the pipeline, only due to the fact that the pipeline was wound with a 200m diameter.

With the deactivation of the extremity clamp that holds the extremities of the Floating Spiral together, the pipeline started to unwind and was restrained by the internal cable system, assuming the configuration presented in Figure 12b. According to this figure, the most tensioned cables at this equilibrium situation were cables 1 and 3, forming two arcs connected by straight sections of pipe. This behavior can be visualized in Figure 15, observing the stresses acting in the pipeline at that moment. The points with the highest curvature and,

therefore, with the highest stresses are located between the free extremity of the pipeline and the point 1 (corresponding to the arc formed by the cable 3) and between the points 2 and 5 (corresponding to the arc formed by the cable 1). The other sections, that assumed a straight configuration, presented almost zero stresses with the exception of the section between the point 5 and the restrained extremity of the pipeline that had not completely assumed a straight configuration.

After that, with the deactivation of cable 1, the pipeline continued to unwind and was restrained again by the internal cable system, assuming the configuration presented in Figure 12c. According to this figure, the most tensioned cables at this equilibrium situation were cables 2 and 3, forming two arcs connected by straight sections of pipe. This behavior can be visualized in Figure 16, observing the stresses acting in the pipeline at that moment. The points with the highest curvature and, therefore, with the highest stresses are located between the free extremity of the pipeline and the point 1 (corresponding to the arc formed by the cable 3), exactly as the last configuration, and between the points 3 and 4 (corresponding to the arc formed by the cable 2). The other sections, that assumed a straight configuration, presented almost zero stresses with the exception of the section between the point 4 and the restrained extremity of the pipeline that had not completely assumed a straight configuration.

With the deactivation of the cable 2, the complete unwinding process of the pipeline was only restrained by the cable 3, assuming the configuration presented in Figure 12d, in which the arc formed by this cable had been stayed unmodified. This behavior can be visualized in Figure 17, observing the stresses acting in the pipeline at that moment. The highest stresses between the free extremity of the pipeline and the point 1 that had been observed in the other figures remain unmodified. As it can be observed in Figure 12d, the pipeline assumed a small curvature from the point 1 to its restrained extremity. It has occurred due to the loss of elastic energy with the pipeline unwinding process. Even with a huge simulation time, the pipeline unwinding velocity was insignificant and insufficient to make that section straight. This was reflected in the stresses graph, which presents an almost linear stress variation from the point 1 to the restrained extremity of the pipeline.

Finally, with the deactivation of the cable 3, the pipeline started to unwind freely, however with a tiny elastic energy. Therefore, for the same reasons that were mentioned in the last paragraph, the simulation time was insufficient to represent the complete unwinding process of the pipeline, which assumed, in the end of the simulation time, the configuration presented in Figure 12e. Again, this small curvature of the pipeline was reflected in the Von Mises stresses graph of Figure 18.

The Figure 19 presents the Von Mises stresses envelope acting along the pipeline. Some disturbance can be observed in this graph that could not be seen in the other figures as this graph considers all the simulation time and thus is affected by transient effects.

The cable tensions due to the unwinding process of the Floating Spiral are illustrated in Figure 20. As it can be observed, the tensions were insignificant in comparison to the cables minimum breaking loads (MBL).

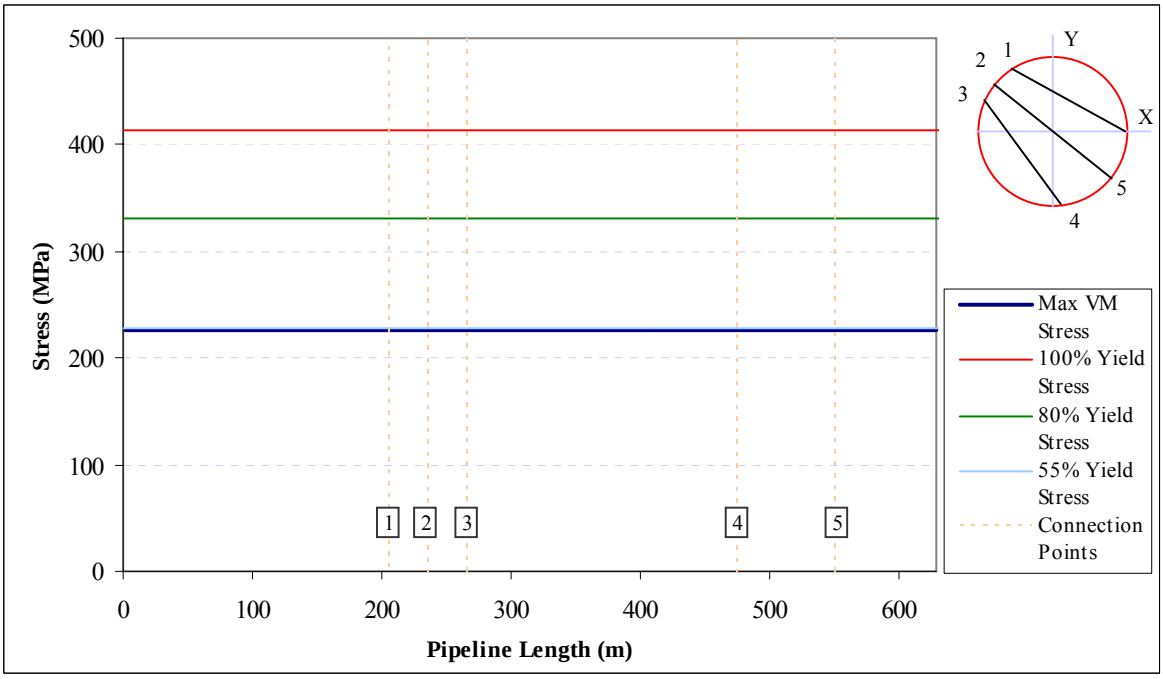

Figure 14: Von Mises stresses at the pipe external wall in the beginning of the numerical simulation (configuration presented in Figure 12a)

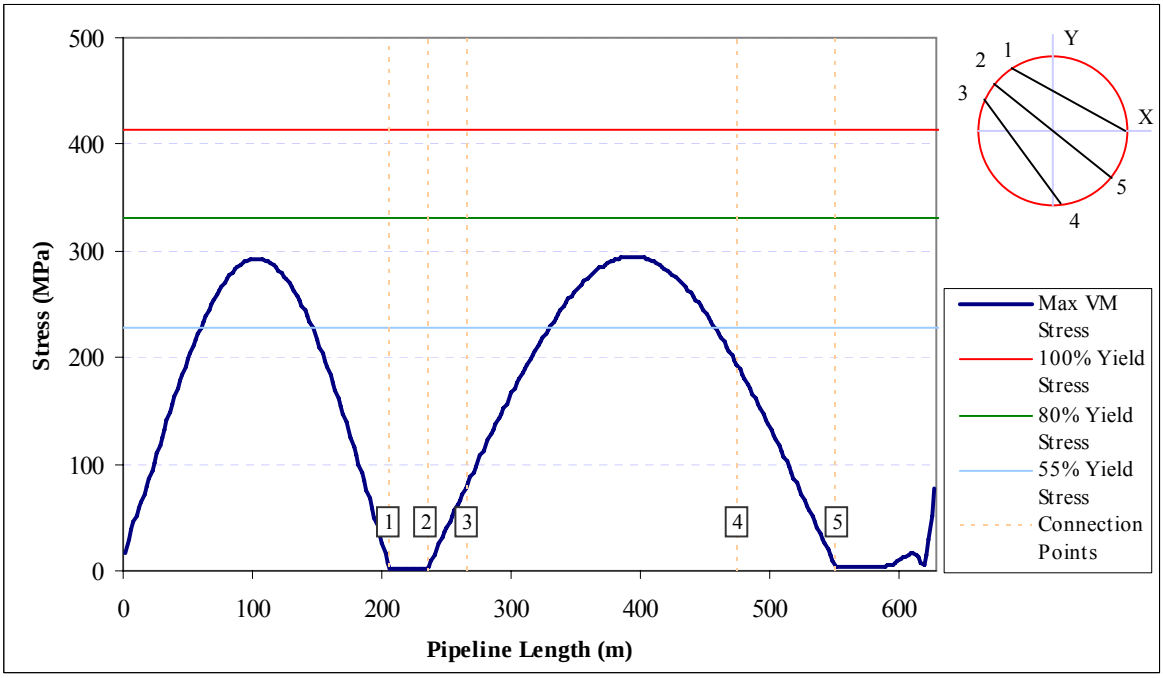

Figure 15: Von Mises stresses at the pipe external wall immediately before the deactivation of cable 1 (configuration presented in Figure 12b)

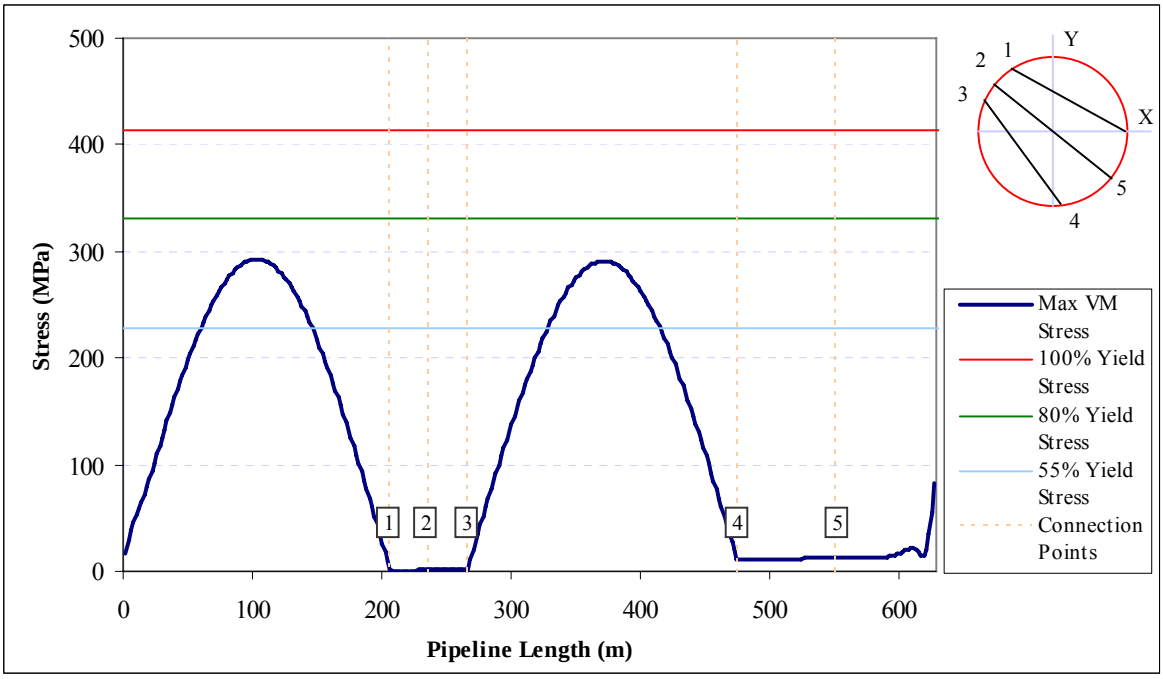

Figure 16: Von Mises stresses at the pipe external wall immediately before the deactivation of cable 2 (configuration presented in Figure 12c)

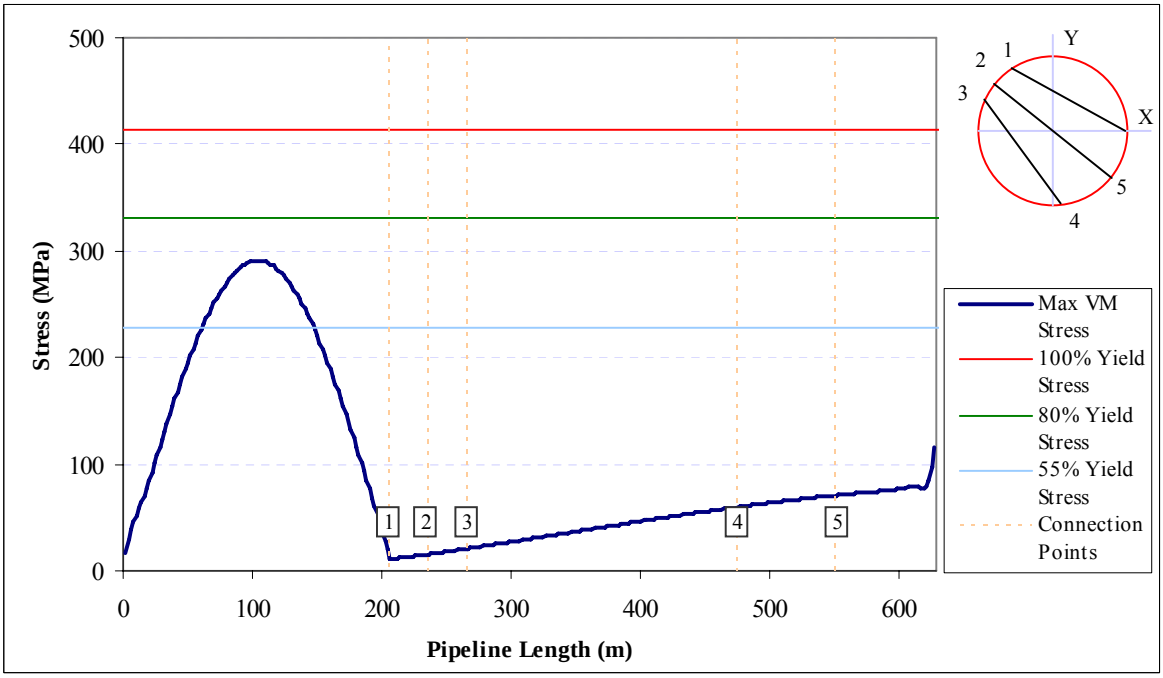

Figure 17: Von Mises stresses at the pipe external wall immediately before the deactivation of cable 3 (configuration presented in Figure 12d)

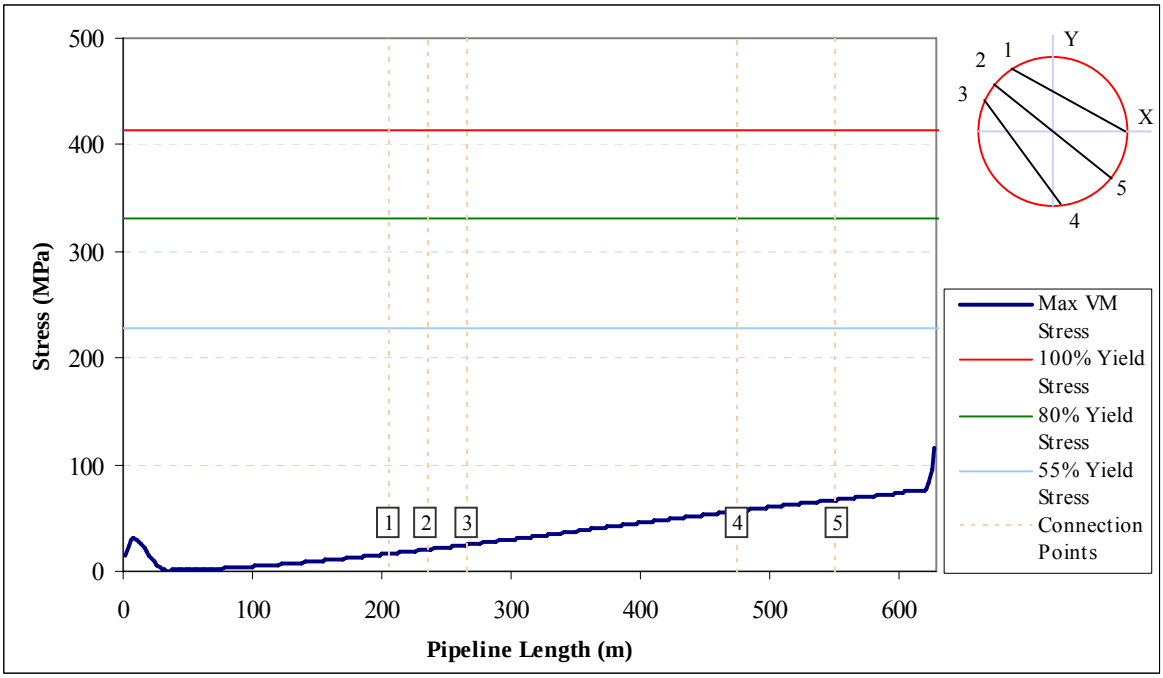

Figure 18: Von Mises stresses at the pipe external wall after 8000s of numerical simulation and the deactivation of all cables (configuration presented in Figure 12e)

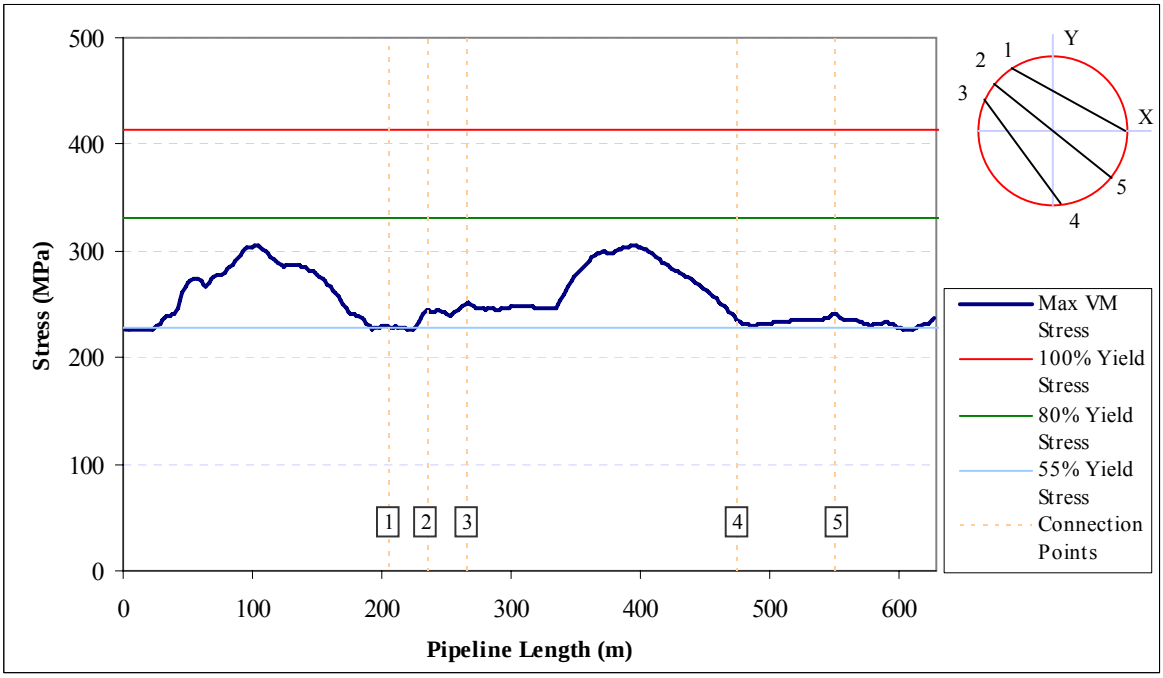

Figure 19: Von Mises stresses envelope at the pipe external wall

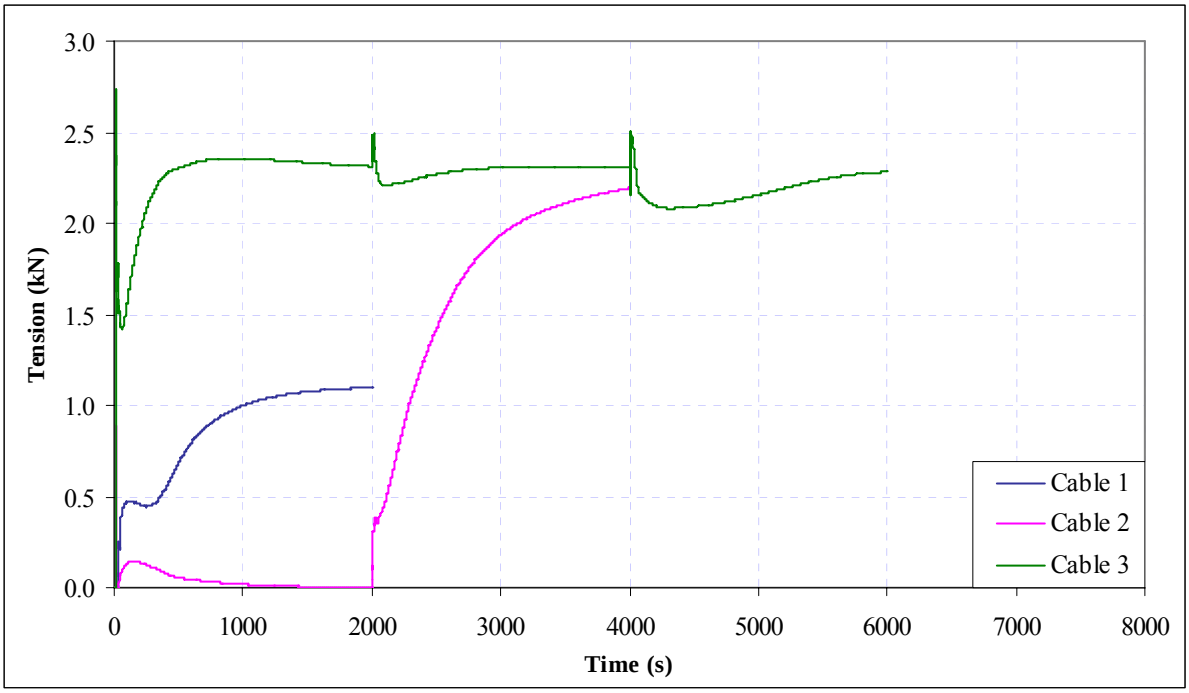

Figure 20: Cable tensions during the numerical simulation

5 FINAL REMARKS

As it can be observed in the sections above, the selective activation of finite elements can be useful for the analyses of several operational procedures and in some emergency situations. It should be emphasized that this is only the first step into the implementation of a robust numerical tool.

Very important analyses could be benefited by numerical simulations evolving from these first results. By adding some features to the numerical tool as, for example, the creation of new elements that did not exist in the beginning of the simulation, other operational procedures could be performed like pipe lay and pull-in analyses.

REFERENCES

API RP 2RD, Design of Risers for Floating Production Systems (FPSs) and Tension-Leg Platforms (TLPs), American Petroleum Institute, 1st Edition, 1998.

API RP 2SK, Recommended Practice for Design and Analysis of Stationkeeping Systems for Floating Structures, American Petroleum Institute, 2nd Edition, 2006.

API Specification 5L, Specification for Line Pipe, American Petroleum Institute, 42nd Edition, 2000.

Bathe, K-J., Finite Element Procedures. New Jersey, Prentice-Hall, 1996.

Jacob, B.P., and Ebecken, N.F.F., An Optimized Implementation of the Newmark/Newton-Raphson Algorithm for the Time Integration of Nonlinear Problems. *Communications in Numerical Methods in Engineering*, vol. 10 pp. 983-992, John Wiley & Sons, UK/USA, 1994.

Jacob, B.P., SITUA-Prosim Program: Coupled Numerical Simulation of the Behavior of Moored Floating Units – Prosim Theory, ver. 3.2 (in Portuguese). LAMCSO/PEC/COPPE, Rio de Janeiro, 2006.

Jacob, B.P., SITUA-Prosim Program: Coupled Numerical Simulation of the Behavior of Moored Floating Units – User Manual, ver. 3.2 (in Portuguese). LAMCSO/PEC/COPPE,

Rio de Janeiro, 2006.

Jacovazzo, B.M., Corrêa F.N., Albrecht, C.H., Jacob, B.P., Torres, F.G.S., and Medeiros, A.R, Numerical Simulation of the "Floating Spiral" Pipeline Installation Procedure: Second Stage, Spiral Transportation, Behavior under Waves. *Proceedings of the 7th International Pipeline Conference – IPC*, September 29-October 3, Calgary, Alberta, Canada, 2008.

Jacovazzo, B.M., and Jacob, B.P., Numerical Tools for the Selective Activation of Finite Elements in the Analysis of Offshore Systems Installation Procedures (in Portuguese). *Proceedings of the 30th Iberian-Latin-American Congress of Computational Methods in Engineering – CILAMCE*, November 8th - 11th, Armação dos Búzios, Brazil, 2009.

Matao, T., Seiji, T., Kunio, T., and Naonosuke, T., A 165 Comparation of Methods for Calculating the Motion of a Semi-Submersible. *Ocean Engineering*, Vol. 12, No. 1. pp. 45-97, 1985.

Morison, J.R., O'Brien, M.P., Johnson, J.W., et al, The Force Exerted by Surfaces Waves on Piles. Petrol. Trans., AIME, no 189, 1950.

Silva, D.M.L., Lima Jr., M.H., Jacob, B.P., Torres, F.G.S., and Medeiros, A.R, Numerical Simulation of the "Floating Spiral" Pipeline Installation Procedure: First Stage, Spiral Assembly. *Proceedings of the 7th International Pipeline Conference – IPC*, September 29-October 3, Calgary, Alberta, Canada, 2008.

Takezawa, S., Hirayama, T., and Morooka, C.K., A Practical Calculation Method of a Moored Semi-Submersible Rig Motion in Waves (On the Effects of Moored Water Depth and Mooring Systems). *Selected Papers From The Journal Of The Society Of Naval Architects And Ocean Engineering Of Japan*, Tokyo,Japão, p. 67-82, 1985.